12 January 2001

ELSEVIER

Chemical Physics Letters 333 (2001) 278–284

CHEMICAL PHYSICS LETTERS

www.elsevier.nl/locate/cplett

Inter-relation between self- and jump-diffusivities in zeolites

D. Paschek, R. Krishna *

Department of Chemical Engineering, University of Amsterdam, Nieuwe Achtergracht 166, 1018 WV Amsterdam, The Netherlands

Received 5 October 2000; in final form 9 November 2000

Abstract

We have performed kinetic Monte Carlo simulations for diffusion of methane, perfluoromethane and 2-methylhexane in silicalite to study the inter-relations between self-, jump- and transport-diffusivities. Both the self- and jump-diffusivities were found to decrease with occupancy, or loading, within the zeolite matrix. Correlation effects cause the self-diffusivity to be lower in value than the jump-diffusivity. Using the Maxwell–Stefan theory for diffusion we derive a simple formula to relate the self- and jump-diffusivities.

1. Introduction

The proper description of diffusive transport within zeolitic materials is of considerable importance in practice because of the many applications in catalytic reaction and separation processes [1–3]. Consider diffusion of a single component (1) within the matrix of a zeolite structure; the molecular flux, expressed in molecules per square meters per second, is given by

$$\mathbf{N}_1 = -\rho D \nabla \Theta_1, \tag{1}$$

where ρ is the density of zeolite matrix, expressed in unit cells per m^3, Θ_1 is the molecular loading, expressed in molecules per unit cell. Eq. (1) defines the transport or Fick diffusivity D. The adsorption isotherm relates the molecular loading Θ_1 to the partial pressure of component 1 in the bulk gas phase surrounding the zeolite crystals, p_1. The Langmuir isotherm gives, for example:

$$\Theta_1 = \frac{\Theta_{1,\mathrm{sat}} b_1 p_1}{1 + b_1 p_1}, \quad \theta_1 \equiv \frac{\Theta_1}{\Theta_{1,\mathrm{sat}}} = \frac{b_1 p_1}{1 + b_1 p_1}, \tag{2}$$

where b_1 is the Langmuir constant, $\Theta_{1,\mathrm{sat}}$ is the saturation loading and θ_1 is the fractional occupancy.

A more fundamental way of describing the diffusion process is to use chemical potential gradients as driving forces:

$$\mathbf{N}_1 = -\rho \Theta_{1,\mathrm{sat}} Đ \left(\frac{\theta_1}{RT} \nabla_{T,p} \mu_1 \right), \tag{3}$$

where Đ is variously referred to as the corrected, jump or Maxwell–Stefan diffusivity [1–4], R is the gas constant and T is the absolute temperature. The transport- and jump-diffusivities are inter-related by

$$D = Đ \Gamma, \tag{4}$$

where Γ is the thermodynamic correction factor [3,4]

$$\Gamma \equiv \Theta_1 \frac{\partial \ln p_1}{\partial \Theta_1} = \theta_1 \frac{\partial \ln p_1}{\partial \theta_1}. \tag{5}$$

* Corresponding author. Fax: +31-20-525-5604.
E-mail address: krishna@its.chem.uva.nl (R. Krishna).

0009-2614/01/$ - see front matter
PII: S0009-2614(00)01363-4

For the Langmuir isotherm (2), the thermodynamic correction factor is given by

$$\Gamma = \frac{1}{1-\Theta_1/\Theta_{\text{sat}}} = \frac{1}{1-\theta_1}. \tag{6}$$

The transport diffusivity D is measured under *non-equilibrium* conditions in which finite gradients of the loading exist. They are determined by macroscopic methods like gravimetry, volumetry, chromatography or frequency response techniques [1,5]. In other experimental procedures, the *self*-diffusivities are measured under *equilibrium* conditions by microscopic techniques, viz. quasielastic neutron scattering and pulsed field gradient NMR. For self-diffusion, the flux of the marked, or tagged, species (1^*) is measured under the influence of the gradient in the loading of marked molecules $\nabla\Theta_{1^*}$ keeping the total molecular loading (tagged and untagged species) constant ($\nabla\Theta_{1^*} + \nabla\Theta_1 = 0$).

$$\mathbf{N}_{1^*} = -\rho D^* \nabla\Theta_{1^*}. \tag{7}$$

In the limit of zero loading the self-, jump- and transport-diffusivities are all identical:

$$Đ = D^* = D; \quad \Theta_1 \to 0. \tag{8}$$

In the published literature, there appears to be no general inter-relation between these three quantities under conditions of finite molecular loadings. In a recent experimental study, Jobic et al. [5] have found that $D > Đ > D^*$ for diffusion of H_2 in NaX zeolite. However, these authors did not provide any theoretical formulae for the inter-relationships. The objective of our Letter is to try to develop a simple mathematical formula relating the three diffusivities using the Maxwell–Stefan theory for diffusion. To validate the developed relations we perform kinetic Monte Carlo simulations of methane, perfluoromethane and 2-methylhexane in silicalite.

2. The Maxwell–Stefan theory of diffusion in zeolites

The essential concepts behind a general constitutive relation for diffusion in multicomponent mixtures were already available more than a century ago following the pioneering works of James Maxwell [6] and Stefan [7]. These ideas have been applied to describe diffusion of n species within a zeolite matrix using the following set of equations [3,4,8–10]:

$$-\rho\frac{\theta_i}{RT}\nabla\mu_i = \sum_{\substack{j=1\\ j\neq i}}^{n} \frac{\Theta_j\mathbf{N}_i - \Theta_i\mathbf{N}_j}{\Theta_{i,\text{sat}}\Theta_{j,\text{sat}}Đ_{ij}} + \frac{\mathbf{N}_i}{\Theta_{i,\text{sat}}Đ_i}; \quad i = 1,2,\ldots,n. \tag{9}$$

In the Maxwell–Stefan formulation for zeolite diffusion, Eq. (9), we have to reckon in general with two types of Maxwell–Stefan diffusivities: $Đ_{ij}$ and $Đ_i$. The $Đ_i$ are the diffusivites which reflect interactions between species i and the zeolite matrix; these correspond to the jump-diffusivities introduced earlier. Mixture diffusion introduces an additional complication due to sorbate–sorbate interactions. This interaction is embodied in the coefficients $Đ_{ij}$. We can consider this coefficient as representing the facility for counter-exchange, i.e., at a sorption site the sorbed species j is replaced by the species i. The net effect of this counter-exchange is the slowing down of a faster moving species due to interactions with a species of lower mobility. Also, a species of lower mobility is accelerated by interactions with another species of higher mobility.

Let us apply the above set of equations Eq. (9) for self-diffusion and consider a system consisting of untagged (1) and tagged (1^*) species; see pictorial representation in Fig. 1. For self-diffusion the conditions of experiment are such that the gradients for diffusion of the tagged and untagged

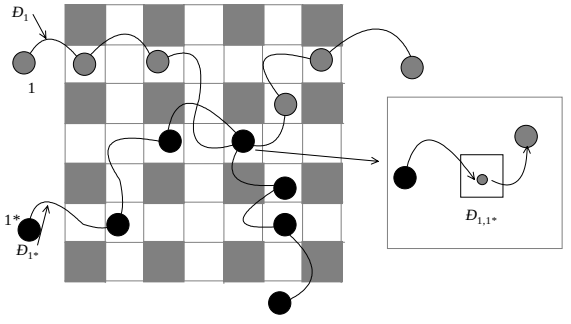

Fig. 1. Pictorial representation of self diffusion using the Maxwell–Stefan diffusion model.

species are equal in magnitude and opposite in sign:

$$\nabla\theta_1 + \nabla\theta_{1^*} = 0 \tag{10}$$

and consequently the fluxes of tagged and untagged species sum to zero:

$$\mathbf{N}_1 + \mathbf{N}_{1^*} = 0. \tag{11}$$

Applying the restrictions (10) and (11) to Eq. (9) we obtain, after imposing $Đ_1 = Đ_{1^*} = Đ$ for the tagged and untagged species:

$$\begin{aligned}\mathbf{N}_1 &= -\rho\Theta_{1,\mathrm{sat}} D^* \nabla\theta_1 \\ &= -\rho\Theta_{1,\mathrm{sat}} \frac{1}{\left(\frac{1}{Đ} + \frac{\theta_1+\theta_{1^*}}{Đ_{1,1^*}}\right)} \nabla\theta_1,\end{aligned} \tag{12}$$

which shows that the tracer diffusivity D^* is

$$D^* = \frac{1}{\left(\frac{1}{Đ} + \frac{\theta}{Đ_{1,1^*}}\right)}, \tag{13}$$

where θ is the total occupancy (tagged and untagged species).

Eq. (13) shows that the tracer, or self-, diffusivity D^* reduces to the Maxwell–Stefan diffusivity only when the interchange coefficient is exceedingly high:

$$D^* \to Đ \quad \text{when } Đ_{1,1^*} \to \infty. \tag{14}$$

In the more general case for finite values of the exchange parameter $Đ_{1,1^*}$ we would expect D^* to be smaller than Đ. As we shall show later in this Letter, the exchange parameter $Đ_{1,1^*}$ is an expression of the *correlation* between the jumps of the tagged and untagged species. A good practical solution would be to take $Đ_{1,1^*} = Đ$; with this assumption we obtain

$$D^* = \frac{1}{\left(\frac{1}{Đ} + \frac{\theta}{Đ}\right)}. \tag{15}$$

We now seek verification of the validity of Eq. (15) by performing kinetic Monte Carlo simulations.

3. Kinetic Monte Carlo simulations

We perform kinetic Monte Carlo (KMC) simulations for diffusion of 2-methylhexane (2MH), methane (CH_4) and perfluormethane (CF_4) at 300 K in silicalite. Each component follows Langmuir isotherm behaviour. We assume the lattice to be made up of equal sized sites which can be occupied by only one molecule at a time and there are no further molecule–molecule interactions. Particles can move from one site to a neighbouring site via hops. The probability per unit time to move from one site to another is determined by transition rates k_{zz} and k_{str} for the zig-zag (zz) and straight (str) channels; see Fig. 2 for a schematic sketch. For 2MH, the transition probabilities were determined based on the calculations of Smit [11] and the procedure is described in detail in our earlier publication [12]. For CH_4 and CF_4, the transition probabilities were chosen to match the Molecular Dynamics simulation results of Pickett [13] and Goodbody [14]. Table 1 lists the input data for the transition probabilities. For 2MH the maximum number of sorption sites per unit cell is 4 and the corresponding number for CH_4 and CF_4 are 24 and 12 respectively. These maximum loadings were taken on the basis of configurational-bias Monte Carlo simulation results of Vlugt et al. [15] and experimental data of Heuchel et al. [16].

We employ a standard KMC methodology to propagate the system (details in Refs. [12,17–19]). A hop is made every KMC step and the system clock is updated with variable time steps. For a given configuration of random walkers on the silicalite lattice a process list containing all possible M moves to vacant intersection sites is created. Each possible move i is associated with a transition probability k_i which is either k_{zz} or k_{str}. Now, the mean elapsed time τ is the inverse of the total rate coefficient

$$\tau^{-1} = k_{\mathrm{total}} = \sum_{i=1}^{M} k_i, \tag{16}$$

which is then determined as the sum over all processes contained in the process list. The actual KMC time step Δt for a given configuration is randomly chosen from a Poisson distribution

$$\Delta t = -\ln(u) k_{\mathrm{total}}^{-1}, \tag{17}$$

where $u \in [0,1]$ is a uniform random deviate. The timestep Δt is independent of the chosen hopping

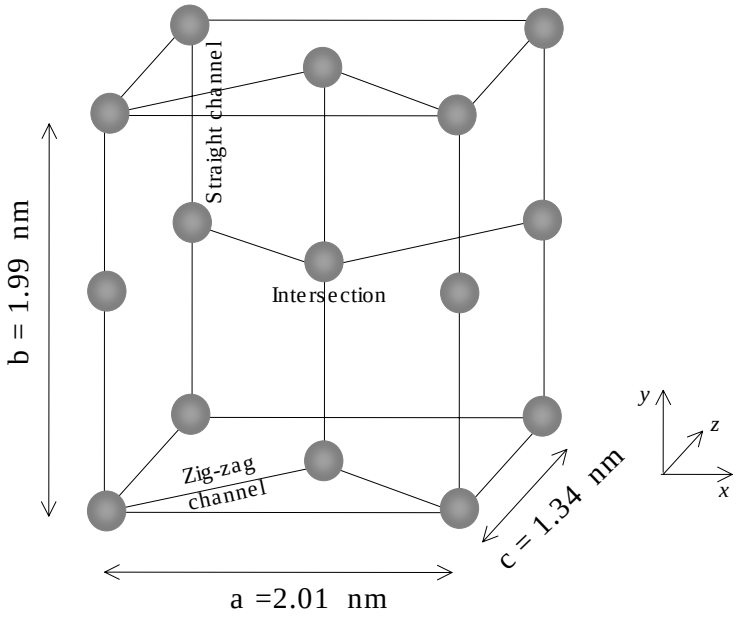

Fig. 2. Diffusion unit cell for silicalite connecting intersection sites (large black dots) via straight and zig-zag channels.

Table 1
Transition probabilities and zero-loading diffusivities

Species	$\Theta_{1,\mathrm{sat}}$	k_{zz} [s^{-1}]	k_{str} [s^{-1}]	Đ(0) [$m^2\ s^{-1}$]
2MH	4	5×10^{4}	1.4×10^{4}	6.86×10^{-14}
CH_4	24	1.8×10^{12}	2.1×10^{12}	1.55×10^{-8}
CF_4	12	2.05×10^{10}	3.25×10^{10}	3.33×10^{-9}

process. To select the actual jump, we define process probabilities according to $p_i = \sum_{j=1}^{i} k_j/k_{\mathrm{total}}$. The ith process is chosen, when $p_{i-1} < v < p_i$, where $v \in [0,1]$ is another uniform random deviate. After having performed a hop, the process list is updated. In order to sample ensemble averages correctly and to calculate dynamical properties more easily, the variable time scale is mapped on a periodic time scale for analysis purposes. In order to avoid surface effects we employ periodic boundary conditions. A choice of $5\times5\times5$ unit cells ensures freedom from finite size effects [12]. About 10^7 simulation steps were performed for each simulation.

The self-diffusivity tensor is described by its components in the x-, y- and z-directions:

$$D_\alpha^* = \lim_{\Delta t\to\infty} D_\alpha^*(\Delta t) = \frac{1}{2}\lim_{\Delta t\to\infty}\frac{1}{\Delta t}\langle r_\alpha^2(\Delta t)\rangle \tag{18}$$

with $\langle\cdots\rangle$ denoting both ensemble and time averaging, r_α is the particle displacement vector and α is x, y or z. Accordingly, the self-diffusion coefficient is expressed by

$$D^* = \frac{1}{3}(D_x^* + D_y^* + D_z^*). \tag{19}$$

Following the works of Reed and Ehrlich [17] and Uebing [20,21] we also calculated the thermodynamic correction factor Γ by relating it to the particle fluctuations in a finite probe volume:

$$\Gamma = \frac{\langle N\rangle}{\langle N^2\rangle - \langle N\rangle^2}, \tag{20}$$

at equilibrium conditions where N is the number of adsorbed particles.

The jump-diffusivities were calculated from the KMC simulations using the following relation [17,20]:

$$Đ = \frac{1}{6}\lim_{\Delta t\to\infty}\frac{1}{\Delta t}\left\langle\left(\frac{1}{N}\sum_{i=1}^{N}(\mathbf{r}_i(t+\Delta t)-\mathbf{r}_i(t))\right)^2\right\rangle, \tag{21}$$

which represents the mean square displacement of the center of gravity of the N adsorbed particles.

4. Verification of Eq. (15)

Let us first consider the KMC simulations for 2MH. Fig. 3a shows the self- and jump-diffusivity obtained from KMC simulations. The jump diffusivity Đ shows a linear dependence on the fractional occupancy:

$$Đ = Đ(0)(1-\theta). \tag{22}$$

The self-diffusivity D^* values from KMC simulations compare very well with the estimations from Eq. (15). The interchange coefficient $Đ_{1,1^*}$ in the Maxwell–Stefan formulation is a reflection of correlation effects which influence the self-diffusion coefficients. The jump-diffusion process is free from such correlation effects [12].

In Fig. 3b the KMC simulations for transport diffusivity D and jump diffusivity Đ, normalised with respect to Đ(0) are presented along with the simulated values of Γ. We note that the KMC simulated Γ follows the theoretical Langmuir behaviour $1/(1-\theta)$. In view of the linear dependence of the jump diffusivity Đ following Eq. (22), the transport diffusivity $D(=Đ\Gamma)$ is independent of the occupancy θ.

The KMC simulation results for CH_4 are shown in Fig. 4. In Fig. 4a the self-diffusivity values in x, y and z directions are presented as a function of the fractional occupancy. These self-diffusivity values are in excellent agreement with the MD simulation results of Goodbody et al. [14]. The self-diffusivity D^*, calculated from Eq. (19), are compared in Fig. 4b with the jump diffusivity Đ from Eq. (15), from MS theory. The jump diffusivity Đ again follows the linear dependence of Eq. (22). The KMC simulations for self-diffusivity D^* for CH_4 show a stronger correlation effect than predicted by Eq. (15). The reason for the stronger correlation effect is to be found in the fact that for methane we have a total of 24 sorption sites compared to only 4 for 2MH. The transport diffusivity for CH_4 is independent of the loading; see Fig. 4c.

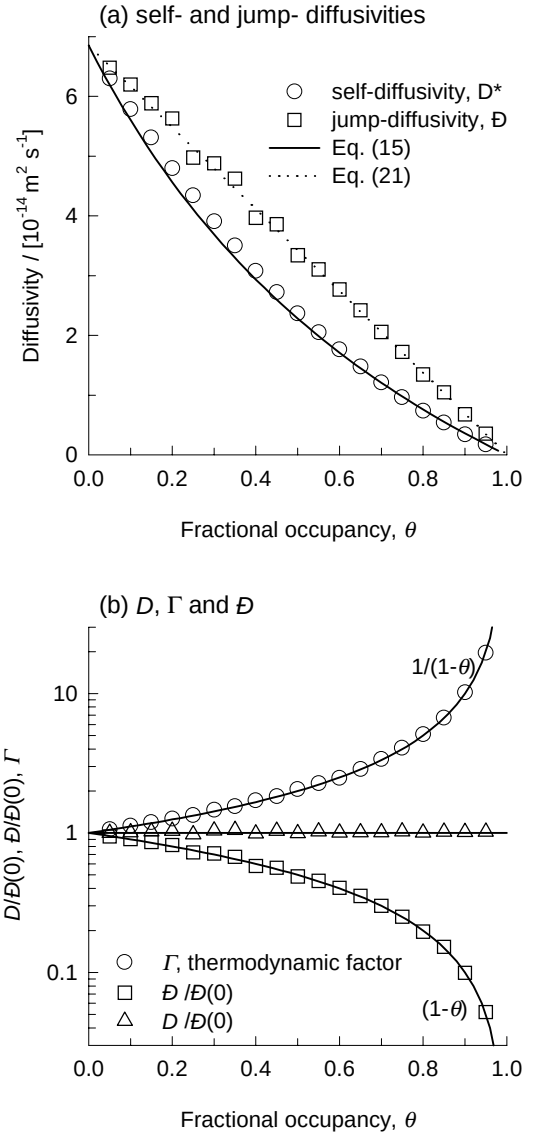

Fig. 3. Monte Carlo simulations of self- and jump- and transport-diffusivities of 2MH in silicalite at 300 K.

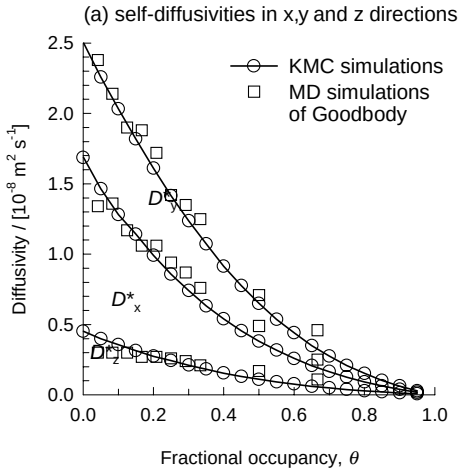

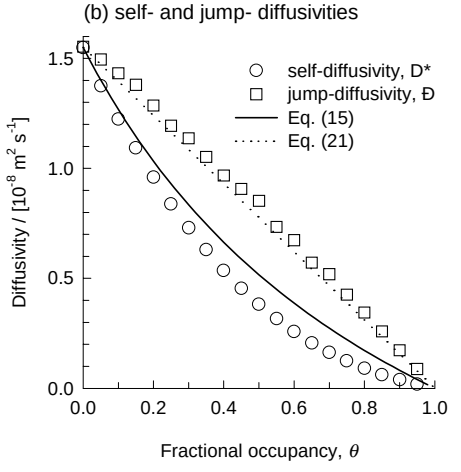

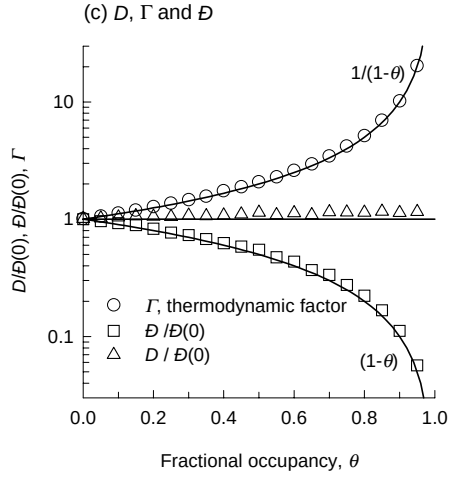

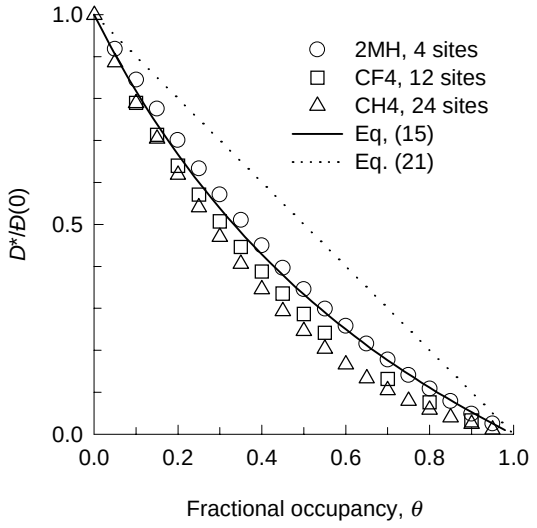

Fig. 5. Comparison of Monte Carlo simulations of self-diffusivities of 2MH, CH_4 and CF_4 in silicalite at 300 K. The self-diffusivities have been normalized with respect to the zero-loading diffusivities $Đ(0)$.

The dependence of correlation effects on the number of sorption sites is emphasised by comparing the (normalised) self-diffusivities for 2MH, CH_4 with that of CF_4, for which the total number of sorption sites is taken to be 12; see Fig. 5. The self-diffusivity values for CF_4 lie in between those for the other two molecules, as is to be expected. It is clear also that the exchange coefficient $Đ_{1,1^*}$ should also take account of the particular system topology with respect to the number of sorption sites. It is not yet clear how such topology effects could be accounted for.

5. Conclusions

Self-diffusivities in zeolites are strongly influenced by correlation effects, whereas the jump- and transport-diffusivities are both free from such

Fig. 4. Monte Carlo simulations of self- and jump- and transport-diffusivities of CH_4 in silicalite at 300 K. In (a) the self diffusivities in x, y and z directions are compared with the MD simulation results of Goodbody et al. [14].

effects. The Maxwell–Stefan diffusion theory has been used to derive a simple formula, Eq. (15), to relate the self-diffusivity to the jump-diffusivity. This formula is found to provide a reasonable representation of the self-diffusivity values obtained from kinetic Monte Carlo simulations. The KMC simulations also show that correlation effects are influenced by the system topology, i.e., the number of sorption sites. Such effects are not accounted for in the continuum Maxwell–Stefan description.

Acknowledgements

The authors acknowledge a grant *Programma-subsidie* from the Netherlands Organisation for Scientific Research (NWO) for development of novel concepts in reactive separations technology.

References

[1] J. Kärger, D.M. Ruthven, Diffusion in Zeolites and other Microporous Solids, Wiley, New York, 1992.
[2] R. Krishna, B. Smit, T.J.H. Vlugt, J. Phys. Chem. A 102 (1998) 7727.
[3] R. Krishna, J.A. Wesselingh, Chem. Eng. Sci. 52 (1997) 861.
[4] R. Krishna, Chem. Phys. Lett. 326 (2000) 477.
[5] H. Jobic, J. Kärger, M. Bée, Phys. Rev. Lett. 82 (2000) 4260.
[6] J.C. Maxwell, Phil. Trans. Roy. Soc. 157 (1866) 49.
[7] J. Stefan, Sitzber. Akad. Wiss. Wien. 63 (1871) 63.
[8] F. Kapteijn, J.A. Moulijn, R. Krishna, Chem. Eng. Sci. 55 (2000) 2923.
[9] R. Krishna, T.J.H. Vlugt, B. Smit, Chem. Eng. Sci. 54 (1999) 1751.
[10] R. Krishna, D. Paschek, Ind. Eng. Chem. Res. 39 (2000) 2618.
[11] B. Smit, L.D.J.C. Loyens, G.L.M.M. Verbist, Faraday Discussions 106 (1997) 93.
[12] D. Paschek, R. Krishna, Phys. Chem. Chem. Phys. 2 (2000) 2389.
[13] S.D. Pickett, A.K. Nowak, J.M. Thomas, B.K. Peterson, J.F.P. Swift, A.K. Cheetham, C.J.J. den Ouden, B. Smit, M.F.M. Post, J. Phys. Chem. 94 (1990) 1233.
[14] S.J. Goodbody, K. Watanabe, D. MacGowan, J.R.P.B. Walton, N. Quirke, J. Chem. Soc. Faraday Trans. 87 (1991) 1951.
[15] T.J.H. Vlugt, R. Krishna, B. Smit, J. Phys. Chem. B 103 (1999) 1102.
[16] M. Heuchel, R.Q. Snurr, E. Buss, Langmuir 13 (1997) 6795.
[17] D.A. Reed, G. Ehrlich, Surf. Sci. 105 (1981) 603.
[18] K.A. Fichthorn, W.H. Weinberg, J. Chem. Phys. 95 (1991) 1090.
[19] C. Saravanan, S.M. Auerbach, J. Chem. Phys. 107 (1997) 8132.
[20] C. Uebing, V. Pereyra, G. Zgrablich, Surf. Sci. 366 (1996) 185.
[21] E. Viljoen, C. Uebing, Surf. Sci. 352–354 (1996) 1007.